

AN INVESTIGATION OF 1,4-DICYANOTETRAZINE
AS A BUILDING BLOCK IN MOLECULE-BASED
MAGNETIC MATERIALS

by

Hoa-Lan Vo

A thesis submitted to the faculty of
The University of Utah
in partial fulfillment of the requirements for the degree of

Master of Science

Department of Chemistry

University of Utah

August 2012

Copyright © Hoa-Lan Vo 2012

All Rights Reserved

The University of Utah Graduate School

STATEMENT OF THESIS APPROVAL

The thesis of Hoa-Lan Vo

has been approved by the following supervisory committee members:

Joel S. Miller , Chair **5/3/2012**
Date Approved

Janis Louie, Member 5/1/2012
Date Approved

Ilya Zharov , Member **5/1/2012**
Date Approved

and by Henry S. White, Chair of
the Department of Chemistry

and by Charles A. Wight, Dean of The Graduate School.

ABSTRACT

Organic ligands are important components in molecule-based magnets, as they allow for control over the physical and magnetic properties. Spin-carrying radical organic ligands, specifically, have been seen to enhance magnetic properties. Investigating reactions of 1,4-dicyanotetrazine, DCNT, an organic ligand capable of being reduced to a radical anion (-0.033 V vs. SCE), with spin carrier and paramagnetic building-blocks such as decamethylferrocene, vanadium hexacarbonyl, and tetrakis(dimethylamino)-ethylene have led to mixed results.

While the reaction of $\text{Fe}(\text{Cp}^*)_2$ with DCNT was expected to form 0-D chains of alternating $[\text{DCNT}]^{\bullet-}$ and $[\text{FeCp}^*_2]^{\bullet+}$ that magnetically ordered, this was not the case as the room-temperature χT value of 0.222 emu K/mol was significantly lower than the calculated spin-only value of 0.75 emu K/mol for a system of two $S = 1/2$ ions. However, as the infrared spectrum indicates reduced DCNT, another bonding motif may be occurring that could include the dimerization or trimerization of DCNT. The structure of $[\text{FeCp}^*_2][\text{DCNT}]$ has not been elucidated and further investigation is needed.

Reaction of DCNT and $\text{V}(\text{CO})_6$ forms a black amorphous precipitate, similar to $\text{V}[\text{TCNE}]_x$. Infrared spectra indicate reduced DCNT; however, the magnet data are inconclusive. TDAE and DCNT forms an electron transfer salt, in which DCNT is reduced and TDAE is oxidized to the 2+ charge. The magnetic data are also inconclusive.

TABLE OF CONTENTS

ABSTRACT	iii
LIST OF FIGURES	v
LIST OF SYMBOLS AND ABBREVIATIONS	vii
ACKNOWLEDGMENTS	x
Chapter	
1. INTRODUCTION TO MAGNETISM AND MOLECULE-BASED MAGNETS.....	1
Introduction and Background on Magnetism	1
Molecule-based Magnets	9
References.....	12
2. SYNTHESIS, STRUCTURE, CHARACTERIZATION OF 1,4-DICYANOTETRAZINE AND INVESTIGATION OF 1,4-DICYANOTETRAZINE-BASED MAGNETIC MATERIALS.....	13
Introduction	13
Experimental	14
Results and Discussion	21
Conclusions	38
References	39

LIST OF FIGURES

<u>Figure</u>	<u>Page</u>
1.1 A diagram showing diamagnetic and paramagnetic behavior.....	3
1.2 An ideal $\chi T(T)$ vs. temperature plot and a diagram of spins showing a) ferromagnetic b) paramagnetic c) antiferromagnetic coupling.....	7
1.3 A plot of $1/\chi(T)$ vs. temperature and examples of paramagnetic, ferromagnetic, antiferromagnetic.....	8
1.4 Common types of ordering seen in magnetic systems.....	9
2.1 Common cyanocarbon acceptors and DCNT a) tetracyanopyrazinide, TCNP b) 7,7,8,8-tetracyano- <i>p</i> -quinodimethane, TCNQ c) R, R'-dicyanoperfluorostilbene, DCPFS d) tetracyanoethylene, TCNE e) 1,4-dicyanotetrazine, DCNT.....	17
2.2 Infrared spectrum of $[\text{FeCp}^*_2][\text{DCNT}]$	25
2.3 Crystal structure of $[\text{FeCp}^*_2]^{*+}[\text{TCNE}]^-$ and crystal structure of $[\text{FeCp}^*_2]^{*+}[\text{TCNQ}]^-$	26
2.4 Infrared spectrum of $\text{V}[\text{DCNT}]_x$	28
2.5 Infrared spectrum of $[\text{TDAE}][\text{DCNT}]$	30
2.6 $\chi T(T)$ and $1/\chi(T)$ for $[\text{FeCp}^*_2][\text{DCNT}]$	31
2.7 $\chi T(T)$ and $1/\chi(T)$ for $\text{V}[\text{DCNT}]_x$	32
2.8 $\chi T(T)$ and $1/\chi(T)$ for $[\text{TDAE}][\text{DCNT}]$	33
2.9 Cyclic voltammograms for DCNT at 100, 400, and 800 mV/s revealing that it undergoes an irreversible one-electron reduction.....	35
2.10 UV-vis spectra of DCNT (●) in MeCN, and 1,2,4,5-tetrazine-3,6-dicarboxamide in DMF (▲) and Nujol (x).....	36

2.11	Atom labeling and thermal ellipsoid plot of DCNT.....	37
2.12	Interleaving herringbone packing motif of DCNT.....	38

LIST OF SYMBOLS AND ABBREVIATIONS

H	applied magnetic field
B	internal magnetic field
M	magnetization
Oe	Oersted
χ	magnetic susceptibility
C	Curie constant
T	temperature
K	Kelvin
N	Avogadro's number
g	Landé g value
S	spin quantum number
μ_B	Bohr magneton
k_B	Boltzmann's constant
J	magnetic exchange parameter
θ	Weiss constant
χ^{-1}	inverse molar susceptibility
T_c	critical temperature
1-D	one-dimensional

2-D	two-dimensional
3-D	three-dimensional
TCNE	tetracyanoethylene
TCNP	2,3,5,6-tetracyanopyrazine
TCNQ	7,7,8,8-tetracyano- <i>p</i> -quinodimethane
TCNB	2,3,5,6-tetracyanobenzene
TCQMI	<i>N</i> ,7,7-tricyanoquinomethanimine
IR	infra red
NMR	nuclear magnetic resonance
QD	quantum design
MHz	megahertz
MPMS	magnetic properties measurement system
SQUID	superconducting quantum interference device
PPMS	physical properties measurement system
h	hour
g	gram
mol	mole
mmol	millimole
emu	electromagnetic unit
H	applied magnetic field
H	hydrogen
s	singlet
d	doublet

t	triplet
THF	tetrahydrofuran
CHCl ₃	chloroform
(P)XRD	(powder) crystal X-ray diffraction
H ₂ SO ₄	Sulfuric acid
UV-Vis	Ultraviolet-visible
[NBu ₄][PF ₆]	tetrabutylammonium hexafluorophosphate
V	volt
mV	millivolt
SCE	standard calomel electrode
M	molar
MeCN	acetonitrile
Fe(Cp*) ₂	decamethylferrocene
TDAE	tetrakis(dimethylamino)ethylene
V(CO) ₆	vanadium carbonyl
V(C ₆ H ₆) ₂	bis(benzene) vanadium
μ _n	bridging to n species, n bridging interactions

ACKNOWLEDGMENTS

I've been fortunate to have a myriad of supporters and mentors during my time as a graduate student at the University of Utah. One of my greatest supporters is my mother, Le. Her continued support of my dreams and goals strengthen as I journey onto the next stage of my adventures.

I would like to thank Dr. Miller for allowing me to join his research group, and making this work possible by providing guidance and wisdom. Because of him, a magnet will never again just be something that sticks to my refrigerator. I must also mention the past and current members of Miller research group Andrew Simonson, Jack DaSilva, Josh Bell, Josh Sussman, Amber McConnell, Jordan Arthur, Preston Erickson, Zach Fox, and Kevin Siegel as they have been great colleagues and friends.

Finally, I would like to thank, the faculty and staff of the University of Utah for their invaluable teachings, and the University of Utah for the support provided by the Graduate Research Fellowship as well as the U.S Department of Energy.

CHAPTER 1

INTRODUCTION TO MAGNETISM AND MOLECULE BASED MAGNETS

Introduction to Magnetism

The study of magnetism has been on going for over a millennia,¹ and is one of the oldest sciences in practice. The phenomenon of magnetism was initially observed by pre-historic man, in which fragments of the mineral magnetite (Fe_3O_4) could attract each other.² By the 12th century AD, there was utilization of Earth's magnetic field for global navigation via a magnetic compass made from lodestone (magnetized Fe_3O_4).² Today, magnets are all around us, from noninvasive visualization of the body's internal organs to magnetic levitation transportation in high speed trains.

A class of magnetic material based on organic molecules, termed “molecule-based magnets,” emerged over two decades ago, and research has expanded in order to study and characterize their structures and magnetic properties. Interest lies in their potential use in switches and sensors, as well as in data storage devices. Molecule-based magnetic material can consist of solely organic components, as well as organic molecules incorporated into structures with metal ions. The use of organic materials in magnets has become popular because it provides a way to tune the magnet's properties by varying the

organic component, as well as avoid the use of rare earth metals, in which the supply is not limitless.

Magnetism is the attractive or repellent of a material due to an applied magnetic field.³ It arises from the fundamental property of electrons referred to as spin. The number, and proximity among electron spins dictate magnetic behavior. When electrons are paired, their spins interact and couple to repel an externally applied field, giving rise to a diamagnetic response.³ Paramagnetism arises from the spin and angular momentum of unpaired electrons interacting with the applied field.³ (Figure 1.1).

As paired electrons make up the inner shells of atoms and molecules, all molecules have a diamagnetic contribution. Hence, a material that has unpaired electrons will have a paramagnetic response in addition to its diamagnetic contributions. The possession of unpaired spins in a material, however, does not make it magnetic. Spins by themselves, or a small number of spins on a molecule will not lead to magnetic ordering. There must be long-range interactions of the unpaired electrons for it to be magnetically ordered.

The measure of a materials response to an applied field is commonly reported as magnetic susceptibility, χ . Diamagnets have a negative susceptibility, which is temperature independent, while paramagnets show a positive and increasing susceptibility as the temperature decreases. Noninteracting spins in a paramagnet obey the Curie Law⁴, where χ , the magnetic susceptibility is related to the Curie constant, C , and inversely related to temperature, T (Equation 1.1). C is defined below (Equation 1.2), where N is Avogadro's number, g is the Lande g-factor, μ_B is the Bohr magneton for an

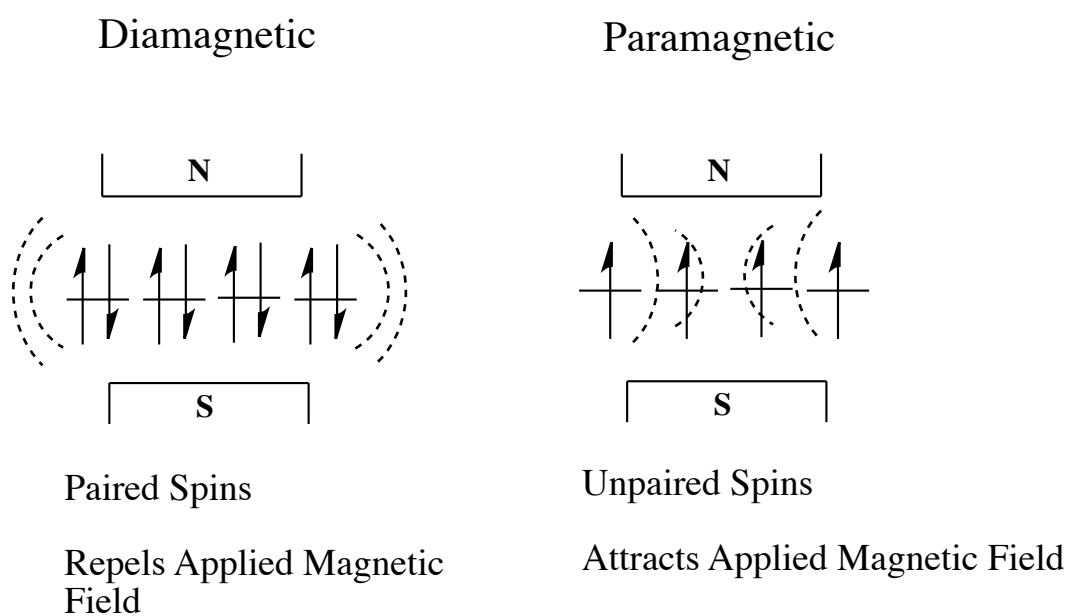


Figure 1.1 A diagram showing diamagnetic and paramagnetic behavior.

electron, S is the quantum spin number, k_B is Boltzmann's constant, and T is temperature in Kelvin.

$$\chi = C / T \quad (1.1)$$

$$C = \frac{Ng^2\mu_B^2S(S+1)}{3k_B} \quad (1.2)$$

The occurrence of spin coupling causes a deviation from ideal paramagnetic behavior. Coupling occurs when the energy, J/k_B , dominates the thermal energy k_B/T . The point at which $J/k_B = k_B/T$ is termed the critical temperature, T_c . Above the critical temperature, the thermal energy is greater than the exchange energy and entropy dominates causing spins to orient randomly. Upon cooling to lower temperatures, thermal energy decreases, and the magnetic exchange energy begins to dominate and spins align, whether parallel or antiparallel, resulting in coupling. Coupling can be determined by referencing the $\chi T(T)$ plot (Figure 1.2). Paramagnetic systems show a flat line, while deviations in a positive or negative manner indicate ferromagnetic or antiferromagnetic coupling.

This coupling is modeled by a modification to the Curie law (Equation 1.3). A quantity called the Weiss constant, θ , is used to modify the Curie law to give the Curie-Weiss law.⁴ (Equation 1.3)

$$\chi = \frac{C}{T - \theta} \quad (1.3)$$

The Weiss constant, θ , indicates the magnitude and type of coupling interactions. It can be determined from the x-intercept of the inverse susceptibility (χ^{-1}) vs.

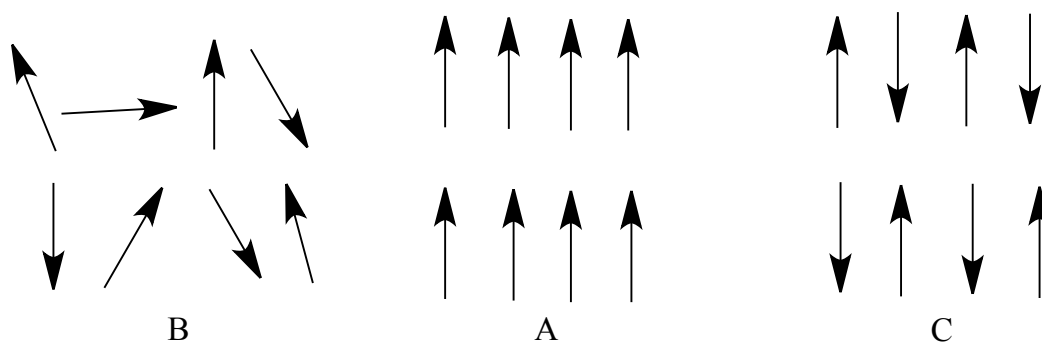
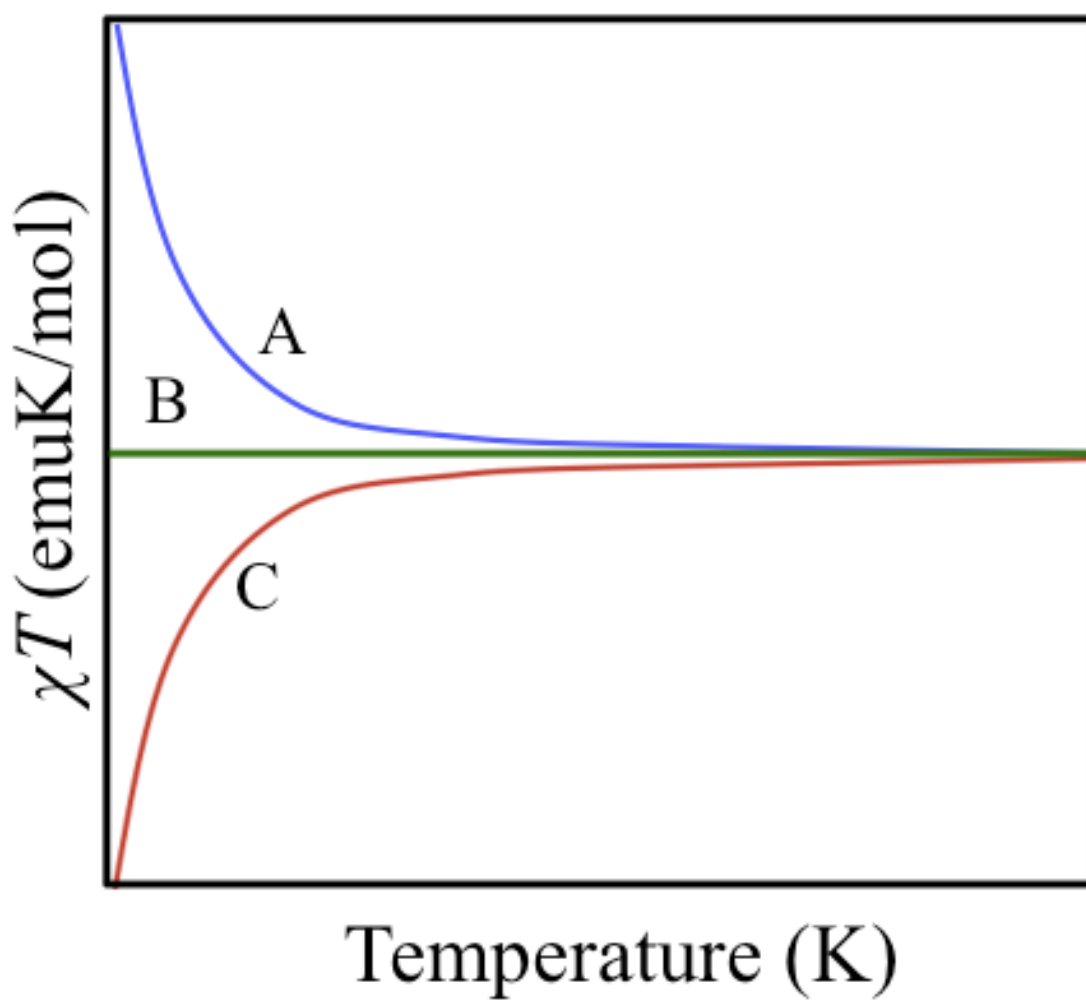


Figure 1.2. An ideal $\chi T(T)$ vs. temperature plot and a diagram of spins showing a) ferromagnetic b) paramagnetic c) antiferromagnetic coupling.

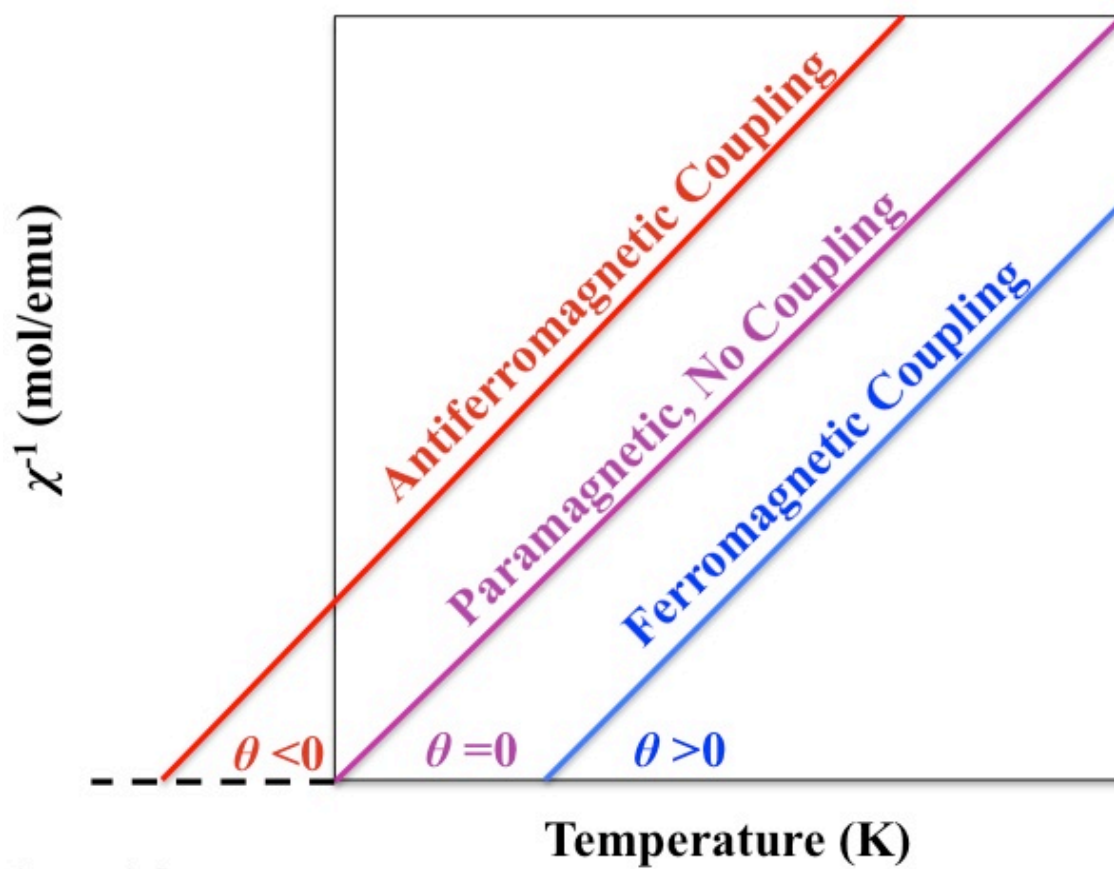
temperature plot (Figure 1.3). A positive θ indicates ferromagnetic interactions, in which the spins are aligned parallel to each other. A true ferromagnet, what we consider a “magnet,” contains spins that are aligned in the absence of an applied field. A negative θ indicates antiferromagnetic interactions, in which the spins are aligned anti-parallel to each other. This results in the system having a net moment of zero, as a result of the spins canceling each other out. Antiferromagnetic interactions are the most common as they arise due to strong overlap of orbitals, leading to greater stability.

Another type of system is a ferrimagnet. The spins in this system align in the same manner as antiferromagnetic systems, however, the spins involved are of inequivalent magnitudes. This results in a net moment along the direction of the larger spin (Figure 1.4).

Molecule-Based Magnets

Magnetic materials are found in a plethora of devices, ranging from hard drives, acoustical equipment, liquid crystal displays (LCDs), and medical imaging devices. More recently, they have been used in Apple Macbooks as a fail-safe device in their power cords. Despite being used in so many different ways, the composition of traditional magnets only vary among a few metals, oxides, and alloys such as Fe, Co, CrO₂, SmO₂, and Ne₂Fe₁₄B.⁵ Their synthesis uses methods such as casting and sintering, which involves high temperatures and pressures, and a strong magnetic field. This makes it difficult to control the structure, which affects the properties of magnets.

Molecule-based magnets are alternative magnetic materials that incorporate organic components, broadening the material’s properties. Many of these properties,



129 20 21

Figure 1.3. A plot of $1/\chi(T)$ vs. temperature and examples of paramagnetic, ferromagnetic, antiferromagnetic coupling.

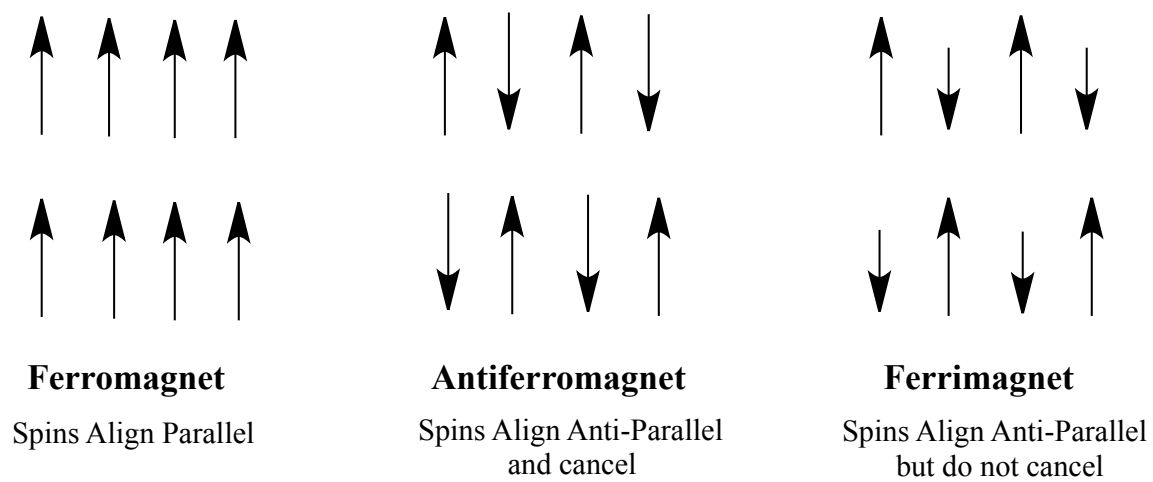


Figure 1.4 Common types of ordering seen in magnetic systems.

not found in traditional magnets, include solubility (in organic solvents), transparency, low temperature utilization, and control over structure (0D-3D networks).⁶ By varying the organic ligand-inorganic network in molecule-based magnets, these magnetic properties can be tuned. Interest lies heavily in the fact that molecule-based magnets can be deposited as thin films via chemical vapor deposition, allowing for the construction of new magnetic devices.⁷

The synthesis of molecule-based magnets is accomplished at ambient pressures and room temperature, making it a more attractive process than the high-temperature and pressure metallurgical process of traditional magnets.⁸ However, molecule-based magnets have low magnetic density due to the diamagnetic organic component. Their applications are also limited, being that most order at very low temperatures due to weak interactions and are air sensitive. For example, some molecule-based materials are found to be pyrophoric,⁸ this may possibly be remedied by applying a coating such as nickel-copper, and parylene.⁹

Molecule-based magnets can be classified into three categories, depending on the role that the organic ligand plays in the structure. One category can be seen in the reaction of an organic ligand, tetracyanoethylene, TCNE, an electron acceptor, and decamethylferrocene, $\text{Fe}(\text{Cp}^*)_2$, an electron donor. Together they form an electron transfer salt, $[\text{FeCp}^*_2]^+[\text{TCNE}]^-$, comprised of a metal/organic radical system, in which decamethylferrocene becomes a metal cationic species and TCNE becomes an organic radical anion¹⁰. The spins of the d and p orbitals interact to give a magnetically ordered system below 4.8K.

The second category of magnetic systems is comprised only of organic radicals. This type of molecule-based magnet is rare, but examples include nitroxides.¹¹ While the synthesis of these magnetic systems is attractive as there is no metal cost, they typically order at low temperatures. In the third category, the organic ligands serve as a framework, bridging and coupling together with paramagnetic metal centers and helping to promote magnetic exchange.¹² An example includes Prussian Blues, in which cyanides link metal centers (V^{II} , Cr^{II} , Mn^{II}) to form 3D networks.¹³ This category of molecule-based magnets is exciting because ordering temperatures can reach as high as 315 K.¹⁴

My research focuses on investigating an organic ligand, 1,4-dicyanotetrazine, and using it to fabricate molecule-based magnets involving the first category. The use of organic compounds in applications regularly reserved for metals is an emerging field of research. The success of $V[TCNE]_x$ as a room-temperature molecule-based magnet, sparked interest in researching other organic cyanocarbon acceptors. Cyanocarbon acceptors are commonly used as building blocks in magnetic systems because the electron-withdrawing nitrile groups stabilize the radicals. The nitrile groups also allow for the formation of 2-D and 3-D arrays as they coordinate to metal cations. Additionally, the unpaired spin on the radical anion can cooperate with spins on the metal sites, leading to enhanced magnetization.

References

- (1) Blackman, M. *Contemp. Phys.* **1983**, *24*, 319.
- (2) Carlin, R. L. *Magnetochemistry*; Springer-Verlag:Berlin, 1986, pp 1-2.
- (3) Drago, R. S. *Physical Methods for Chemists*, 2nd Ed.; Saunders College Publishing: San Francisco, 1992; Chap. 11.
- (4) Kahn, O. *Molecular Magnetism*; VCH Publishers Inc.: New York, NY, 1993, pp 1-17.
- (5) (a) Miller, J. S. *Inorg. Chem.* **2000**, *39*, 4392. (b) *Magnetism: Molecules to Materials I-IV*, Miller, J. S. and Drillon, M. Eds., Wiley-VCH, Weinheim, New York, **2001-2002**. (c) Yoshihara, D.; Karasawa, S.; Koga, N. *J. Am. Chem. Soc.*, **2008**, *130*, 10460. (d) Stickley, K. R.; Selby, T. D.; Blackstock, S. C. *J. Org. Chem.*, **1997**, *62*, 448.
- (6) (a) Bagnato, J. D.; Miller, J. S. *J. Phys. Chem. C* **2010**, *114*, 20614. (b) Fujisaki, T.; Nakazawa, Y.; Oguni, M.; Nakata, K.; Yamashita, M.; Lecren, L.; Miyasaki, H. *J. Phys. Soc. Jpn.* **2007**, *76*, 105602/1. (c) Stone, K. H.; Stephens, P. W.; McConnell, A. C.; Shurdha, E.; Pokhodnya, K. I.; Miller, J. S. *Adv. Mater.* **2010**, *22*, 2514.
- (7) Erickson, P. K.; Miller, J. S. *J. Magn. Magn. Mater.* **2012**, *324*, 2218–222.
- (8) Manriquez, J. M.; Yee, T. G.; Mclean, R. S.; Epstein, A. J.; Miller, J. S. *Science*. **1991**, *252*, 1415-1416.
- (9) Noar, J.H.; Wahab, A.; Evays, R. D.; Wojcik, A. G. *Euro. J. Orth.* **1999**, *21*, 685-693.
- (10) Miller, J. S.; Calabrese, J. C.; Rommelmann, H.; Chittipeddi, S. R.; Zhang, J. H.; Reiff, W. M.; Epstein, A. J. *J. Am. Chem. Soc.* **1987**, *109*, 769-781.
- (11) (a) Sugano, T.; Kurmoo, M.; Uekusa, H.; Ohashi, Y.; Day, P. *J. Solid State Chem.* **1999**, *145*, 427. (b) Train, C.; Norel, L.; Baumgarten, M. *Coord. Chem. Rev.* **2009**, *253*, 2342.
- (12) *Magnetism: Molecules to Materials I-IV*, Miller, J.S. and Drillon, M. Eds. Wiley-VCH, Weinheim, New York, **2001-2002**.
- (13) (a) Ohkoshi, S.-i.; Hashimoto, K. *Phys. Rev. B* **1999**, *60*, 12820. (b) Tokoro, H.; Ohkoshi, S. *Dalton Trans.* **2011**, *40*, 6825. (c) Earnshaw, A.; Hewlett, P.C.; King, E. A.; Larkworthy, L.F. *J. Chem. Soc. A* **1968**, 241.

- (14) (a) M. Verdaguer et al. *Coord. Chem. Rev.* **1999**, *190*, 1023–1047. (b) Ferlay, S.; Mallah, T.; Ouahes, R.; Veillet, P.; Verdaguer, M. *Nature*, **1995**, *378*, 701–703.

CHAPTER 2

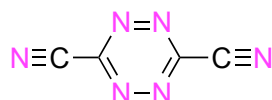
SYNTHESIS, STRUCTURE, CHARACTERIZATION OF 1,4-DICYANOTETRAZINE AND INVESTIGATION OF 1,4-DICYANOTETRAZINE-BASED MAGNETIC MATERIALS

Introduction

Organic radicals have gained attention for their ability to enhance communication between metal centers, making them popular building blocks for molecule-based magnets. Organic electron acceptors, especially, have gained attention for their ability to produce magnetic systems. One such acceptor is tetracyanoethylene, TCNE^{•-}, a radical anion (Figure 2.1d). It has been used extensively due to the fact that it has a low reduction potential [$E_{1/2}^0 = 0.15$ V vs. SCE], and nitrile groups that can coordinate to metals ions.¹ The contribution of its spin, $S=1/2$, to magnetic systems allows for a pathway for metal spin sites to communicate with each other.

Tetracyanoethylene was used to synthesize the first organic-based magnet, $[\text{FeCp}^*_2]^{2+}[\text{TCNE}]^{\bullet-}$, found to ferromagnetically order to 4.8 K.² Subsequently, a room temperature magnet was synthesized via bis(benzene)vanadium, $\text{V}(\text{C}_6\text{H}_6)_2$, or vanadium hexacarbonyl, $\text{V}(\text{CO})_6$, and TCNE.³ Since then, scientists have been investigating

acceptors in order to enhance and control magnetic properties. Focus has been on other polynitrile species (Figure 2.1) such as R,R'-dicyanoperfluorostilbene (DCPFS), tetracyanopyrazinide (TCNP), and 7,7,8,8-tetracyano-p-quinodimethane (TCNQ). Reactions of these cyanocarbon accepts with $V(CO)_6$ and $V(C_6H_6)_2$ have yielded magnets that order from 7.5 K to 205 K.¹



DCNT

1,4-dicyanotetrazine, DCNT, has been identified as a new acceptor for organic-based magnets. With nitrile groups on the 1,4 position, DCNT has potential coordinating sites for bonding to two metal centers. The tetrazine core has a low-lying π^* molecular orbital, due to the presence of electronegative nitrogens, allowing for the facile formation of radical anions.⁵ In addition, with a reported reversible one-electron reduction at -0.094 V vs. SCE,⁶ it has potential to stabilize magnetically ordered organic-based magnets. While $V(CO)_6$ [$E^{1/0} = +0.88$ V vs. SCE],⁷ should not be able to reduce DCNT, much like with TCNP and TCNQ, $V(DCNT)_x$ is anticipated to form via the same associative reaction of $V(CO)_6$.⁸ Herein the synthesis of 1,4-dicyanotetrazine, its structure, and redox chemistry via decamethylferrocene, tetrakis(dimethylamino)ethylene, and vanadium carbonyl will be discussed.

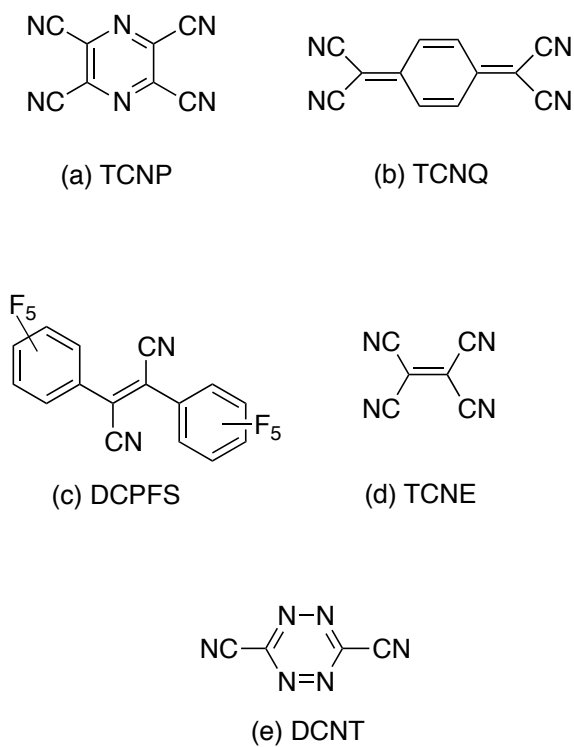


Figure 2.1. Common cyanocarbon acceptors and DCNT a) tetracyanopyrazinide, TCNP b) 7,7,8,8-tetracyano-*p*-quinodimethane, TCNQ c) R, R'-dicyanoperfluorostilbene, DCPFS d) tetracyanoethylene, TCNE e) 1,4-dicyanotetrazine, DCNT.⁴

Experimental

General Methods

All chemicals used in the preparation of 1,4-dicyanotetrazine were used as received. The starting material, ethyl ester hydrochloride, was purchased from Alfa Aesar. Decamethylferrocene (Arcos Organics) and tetrakisdimethylaminoethylene (Sigma-Aldrich) were purchased and used without purification. $\text{V}(\text{CO})_6$ was synthesized from $[\text{NEt}_4][\text{V}(\text{CO})_6]$ following a literature procedure.⁹

Infrared spectra were taken using a Bruker Tensor 37 FTIR spectrophotometer with $\pm 1 \text{ cm}^{-1}$ resolution, and scanned in the range of 400 - 4000 cm^{-1} . UV/Visible spectroscopy was carried out on a Hitachi U4100 UV-vis-Near IR Spectrometer, scanning from 190 to 820 nm. Samples were prepared as 0.1 M solutions in MeCN in 1 mL quartz cuvettes.

Cyclic voltammograms were performed with a Bioanalytical Systems Inc. Model MF-9092 Epsilon Instrument scanning from +0.0 to -0.75 V with scan rates of 100 to 800 mV/s. Platinum working and counter electrodes were used with a Ag/AgCl charged with $[\text{NBu}_4][\text{PF}_6]$ reference electrode and $[\text{NBu}_4][\text{PF}_6]$ supporting electrolyte in acetonitrile (0.10 M). All CV's were referenced to a ferrocene/ferrocenium standard and are reported vs. SCE. All measurements were carried out in a glovebox.

Magnetic susceptibility measurements were made between 2 and 300 K using a Quantum Design MPMS-5XL 5 T SQUID magnetometer equipped with a reciprocating sample measurement system; or using a Quantum Design PPMS-9 AC/DC susceptometer. Magnetic studies were conducted in a gelatin capsule. Diamagnetic corrections were made for both the sample and gelatin cap sample holder.

Synthesis

1,4-dicyanotetrazine was synthesized via a modified method from the literature¹⁰ in seven linear steps (Scheme 2.1), starting with the commercially available glycine ethyl ester hydrochloride.

Ethyl diazoacetate (**B**)

A 3-neck, 500 mL round bottom flask equipped with a magnetic stir bar was charged with water (150 mL), glycine ether ester hydrochloride (**A**) (140 g, 1.00 mol), sodium acetate (3 g) and cooled in an ice bath. The reaction was allowed to stir, followed by the addition of a cold solution of sodium nitrite (80 g, 1.15 mol) in water (100 mL) and ethyl ether (100 mL). Sulfuric acid (16.7 mL, 10%) was slowly added dropwise until bubbling ceased. The reaction was then quickly poured into a large separatory funnel, the bottom layered was returned to the reaction flask, and the ether layer was washed with a cold sodium carbonate solution and dried with magnesium sulfate.

A second portion of ether (100 mL) was added to the reaction flask and the procedure was repeated two more times. The ether layers were combined and concentrated via a rotary evaporator to give ethyl diazoacetate (**B**) as a yellow oil (105, 91%). NMR (CDCl₃) δ 4.26 (s, 2H), 4.13 (q, 2H), 1.53 (s, 2H), 1.29 (t, 3H)

Disodium dihydro-1,2,4,5-tetrazine-3,6-dicarboxylate (**C**)

A solution of sodium hydroxide (160 g, 4 mol) in 250 mL of water was stirred at 60° C while ethyl diazoacetate (100 g, 875 mmol) (**B**) was added dropwise. After

approximately one hour, the reaction slurry was cooled to room temperature and washed with one liter of 95% ethanol five times. The precipitate was collected by filtration, washed with 500 mL absolute ethanol and 500 mL anhydrous ether, and dried in air to give disodium-dihydro-1,2,4,5-tetrazine-3,6-dicarboxylate (**C**) as a yellow-brown solid (83 g, 88%). NMR (CDCl_3) δ 7.1 (s, 2H)

Dihydro-1,2,4,5-tetrazine-3,6-dicarboxylic acid (D)

A solution of **C** (75 g, 0.35 mol) in 85 mL of water and crushed ice (83 g) was cooled with a sodium chloride bath while a solution of concentrated hydrochloric acid, HCl, (70 mL of 36-38%) was added dropwise, with stirring. The reaction mixture was extracted five times with anhydrous ether, filtered, and dried under reduced pressure to give dihydro-1,2,4,5-tetrazine-3,6-dicarboxylic acid (**D**) (41 g, 69%). NMR (CDCl_3) δ 7.1 (s, 2H), 10.78 (s, 2H).

Dimethyl-dihydro-1,2,4,5-tetrazine-3,6-dicarboxylate (E)

Thionyl chloride (32 mL, 0.466 mol) was slowly added to a chilled (-30°C) solution of absolute methanol (600 mL). **D** (38 g, 221 mol) was added in small portions over 30 min to the cooled solution. The reaction mixture was then warmed to room temperature and subsequently warmed to 35°C for 2 h. The reaction mixture was cooled and the precipitate was collected by filtration. The solid was washed with ether and titrated with dichloromethane while the filtrate was concentrated to give an orange-brown oil. The orange-brown oil was extracted with dichloromethane six times. The combined dichloromethane extracts and titrate were dried with magnesium sulfate and

concentrated to give dimethyl dihydro-1,2,4,5-tetrazine-3,6-dicarboxylate (**E**) (20 g, 45%). NMR (CDCl₃) δ 7.1 (s, 1H), 3.68 (s, 6H).

Dihydro-1,2,4,5-tetrazine-3,6-carboxamide (F)

E (17 g, 85 mmol), was dissolved in concentrated ammonium hydroxide (200mL) and ammonium chloride (1.70 g). The mixture was allowed to stir at room temperature for 12 h. The resulting dihydro-1, 2,4,5-tetrazine-3, 6-dicarboxamide (**F**) was filtered and washed with water and ethanol to give a yellow solid (14.1 g, 98%). NMR (CDCl₃) δ 7.1 (s, 2H), 7.68 (s, 4H).

1,2,4,5-tetrazine-3,6-dicarboxamide (G)

F (7 g, 41 mmol) was added to 500 mL of water and chilled to 0° C to give a yellow slurry. A stream of nitrous gas was bubbled directly into the reaction mixture, producing a yellow to hot pink color change. The nitrous gas was produced in a separate round bottom flask via the disproportionation of nitrous acid. To the separate 3-neck 250 mL round bottom flask, equipped with a nitrogen inlet, and an outlet tube to the reaction flask, concentrated hydrochloric acid (100 mL, 38%) was added dropwise to a solution of sodium nitrite (50 g) in water (150 mL). The reaction was filtered and dried to afford 1,2,4,5-tetrazine-3,6-dicarboxamide (**G**) (5.68 g, 82%). IR (KBr/cm⁻¹): ν_{NH} 3407 s, 3186 s ν_{CO} 1673 s.

1,4-dicyanotetrazine

A ground mixture of **F** (1 g, 6mmol) and phosphorus pentoxide (5 g, 35 mmol) was heated at 160° C in vacuo in a sublimation apparatus at 10^{-4} torr via an oil diffusion pump. The sublimed product was further purified by an additional sublimation in vacuo at 60° C to give pure 1,4-dicyanotetrazine as orange-red crystals (100 mg, 10%). IR (KBr/cm⁻¹): $\nu_{\text{C}\equiv\text{N}}$ 2271 m, 1345 s, 1281 w, 904 m, 850 m, 810 w, 588 s, 515 m.

[Fe^{III}Cp*₂]⁺⁺[DCNT]⁻

[Fe^{III}Cp*₂]⁺⁺[DCNT]⁻ was synthesized by adding one equivalent of DCNT, (57 mg, 0.43 mmol) dissolved in 5 mL of tetrahydrofuran, THF, dropwise to an equivalent of Fe(Cp*)₂ (140.8 mg, 0.43 mmol) dissolved in 5 mL THF in a glove box. This resulted in an immediate color change to a dark green. The reaction was allowed to stir for 30 min and was precipitated at -20°C. A green precipitate collected via filtration [yield 16.2 mg, 83%] Crystals suitable for single crystal X-ray diffraction could not be obtained. IR (KBr; cm⁻¹): ν_{CN} 2222 s, ν_{CH} 1476 s, 1385 s, 1300 s. A powder sample was sent off for powder X-ray diffraction.

[TDAE]²⁺[DCNT]₂⁻

[TDAE]²⁺[DCNT]₂⁻ was synthesized by adding two equivalents of DCNT, (35.8 mg, 0.27 mmol) dissolved in acetonitrile, drop wise to one equivalent of TDAE (25.9 mg, 0.13 mmol) dissolved in 5 mL acetonitrile in a glove box. Upon addition there was no immediate color change. The reaction was allowed to stir for 30 min and was crystallized

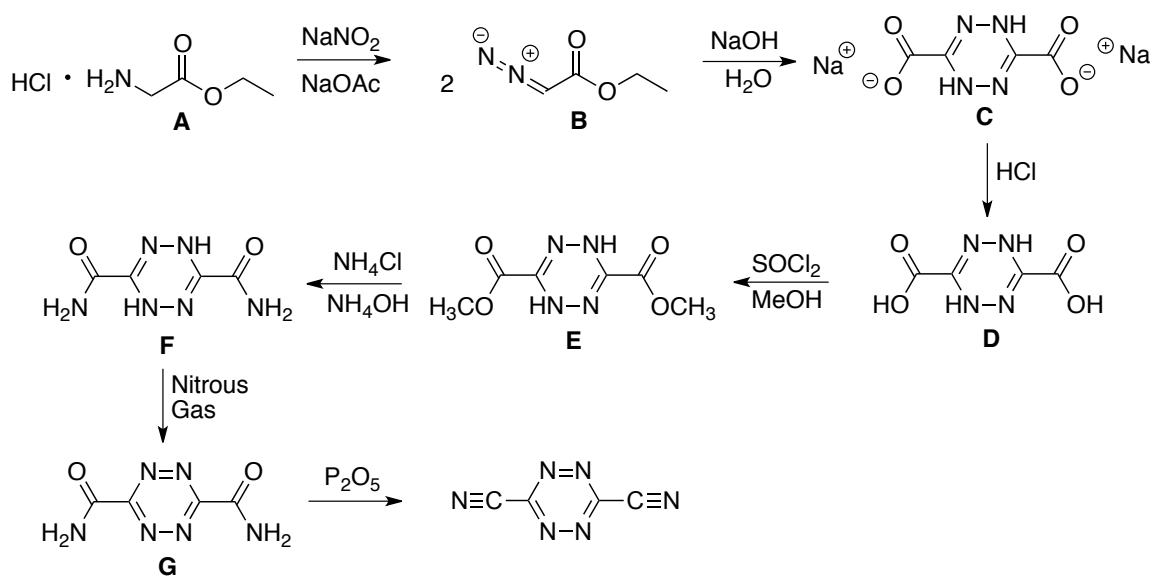
in a -20°C freezer. The next day, a grey-light pink precipitate was filtered, washed and dried under vacuum. [Yield 46 mg, 74%] IR (KBr; cm^{-1}): ν_{CN} 2222 s, 1669 s, 1652 s, ν_{CH} 1409 s, 1399 s, 1386 s. A vial of the material was sent off for powder X-ray diffraction.

V[DCNT]•zCH₂Cl₂

DCNT (37.3mg, 0.28 mmol) was dissolved in 5 mL of CH₂Cl₂, V(CO)₆ (31mg, 0.14 mmol) was dissolved in 5 mL of CH₂Cl₂ and each solution was filtered. The solution of V(CO)₆ was drop wise added to the solution of DCNT, with stirring. Upon addition the solution immediately turned black and a black precipitate formed. Bubbles also formed due to carbon monoxide evolution. After the addition was completed, the reaction was stirred for 15 min with occasional venting and then stirred overnight. The next day, the dark precipitate was filtered, washed, and dried under vacuum. [Yield 0.039 mg, 88%] IR (KBr; cm^{-1}): ν_{CN} 2222 b, 1578 s, 1487 s.

Results and Discussion

As the search for new organic components that provide both spin and spin coupling to stabilize magnetic ordering, we seek to bring DCNT and its reduction to light. With the goal of reducing DCNT, studying the reduced structure, and forming new organic-based magnet material, it was reacted with decamethylferrocene, vanadium carbonyl, tetrakis(dimethylamino)ethylene, and manganese tetraphenylporphyrin. While the literature reports a reversible reduction potential,⁶ DCNT was experimentally found to possess an irreversible reduction potential. Hence it is hypothesized that the radical anion is unstable and will unlikely lead to new molecule-based magnets.



Scheme 2.1. Synthesis of 1,4-dicyanotetrazine.

Spectroscopic studies

1,4-dicyanotetrazine, DCNT, possesses a ν_{CN} peak at 2271 cm^{-1} , and a sharp $\nu_{\text{C}=\text{N}=\text{N}}$ peak at 1345 cm^{-1} corresponding to the tetrazine core. Reaction of DCNT with $\text{Fe}(\text{Cp}^*)_2$ in tetrahydrofuran, THF, yielded a green precipitate that exhibited one sharp ν_{CN} absorption at 2222 cm^{-1} , and ν_{CH} bands 1476 s , 1385 s , 1300 s cm^{-1} (Figure 2.2). The clean 2222 cm^{-1} ν_{CN} IR absorption indicated the presence of reduced DCNT, as these absorptions are lower in frequency than neutral DCNT at 2271 cm^{-1} . The same ν_{CN} shifts to lower frequency is seen in the reduction of TCNE and TCNQ.^{9,11}

The first organic-based magnet was comprised of the electron transfer salt of $[\text{FeCp}^*_2]^{++}[\text{TCNE}]^{\bullet-}$, which orders ferromagnetically at 4.8 K. Its structure and magnetic behavior have recently been elucidated,¹² as well as other products of cyanocarbon acceptors (TCNQ, TCQMI)^{19,13} with decamethylferrocene. Members of this family of compounds has the same structural motif of parallel chains, alternating between organic radical anions and $[\text{Fe}(\text{Cp}^*)_2]^+$ cations (Figure 2.3). As DCNT is in the same class of compounds and an IR spectrum in the nitrile region-indicated a complete reduction of the compound, it is hypothesized that the reaction between DCNT and $\text{Fe}(\text{Cp}^*)_2$ similarly forms a chain of $[\text{Fe}^{\text{III}}\text{Cp}^*_2]^{++}[\text{DCNT}]^{\bullet-}$.

The reaction of DCNT and $\text{V}(\text{CO})_6$ in CH_2Cl_2 yielded a black amorphous product that exhibited a broad ν_{CN} absorption at 2220 and 2195 cm^{-1} (Figure 2.4). The ν_{CN} IR absorptions, similar to that observed for $[\text{Fe}(\text{Cp}^*)_2][\text{DCNT}]$ product, are lower in energy than neutral DCNT, 2271 cm^{-1} , and can be indicative of reduced DCNT. The broadness of the ν_{CN} stretch suggests that there are multiple CN environments in the material. It is expected that the reaction between DCNT and $\text{V}(\text{CO})_6$ should proceed as in Equation 2.1:

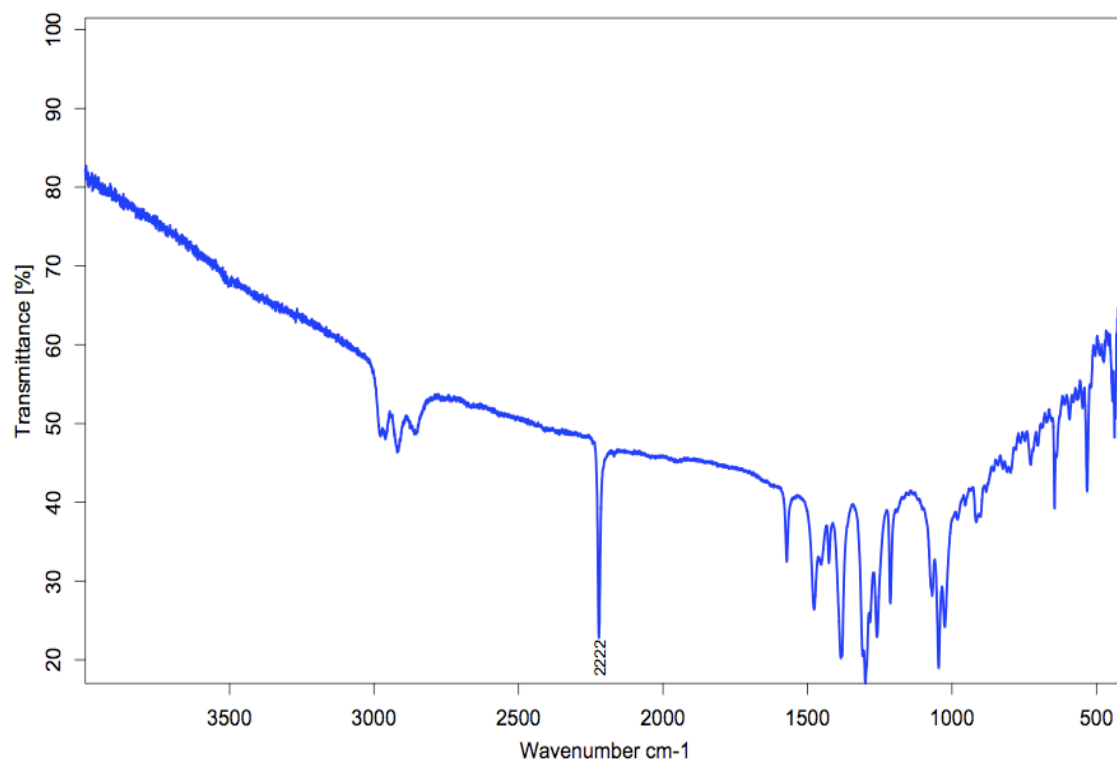


Figure 2.2. Infrared Spectrum of $[\text{FeCp}^*_2][\text{DCNT}]$

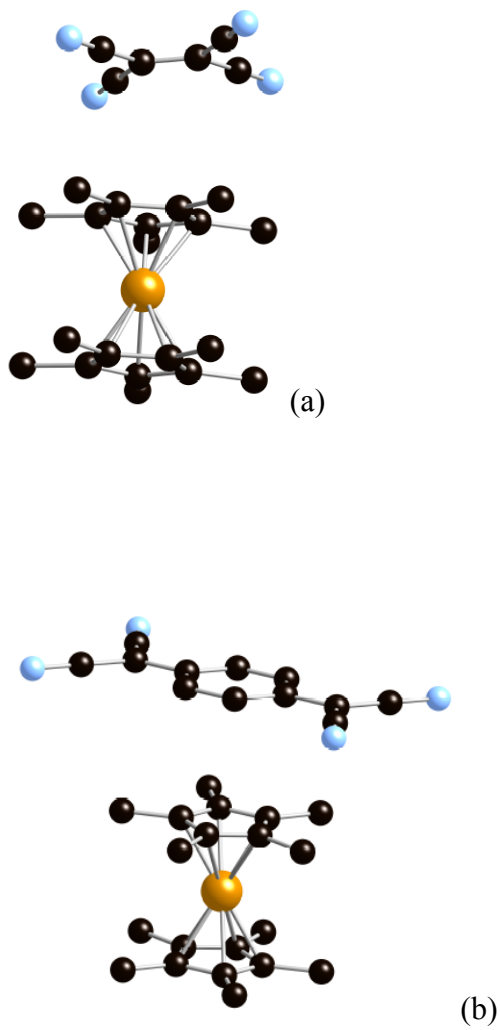
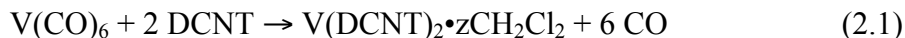


Figure 2.3. a) crystal structure of $[\text{FeCp}^*_2]^+[\text{TCNE}]^-$ b) crystal structure of $[\text{FeCp}^*_2]^+[\text{TCNQ}]^-$.¹¹



Evidence of $\text{V}(\text{DCNT})_2 \cdot \text{zCH}_2\text{Cl}_2$ forming is supported experimentally by the evolution of carbon monoxide during addition of DCNT into a solution of $\text{V}(\text{CO})_6$. As well as in the product IR spectrum, which shows a broad ν_{CN} absorptions shifted to lower energy.

Of the cyanocarbon/metal materials investigated to date, $\text{V}^{\text{II}}(\text{TCNE})_2$ exhibits the highest critical temperature ($>350 \text{ K}$). Since the structure is unknown, due to a possible source of disorder having to do with the coordination environment of the metal, investigation into other cyanocarbon acceptors and their reactions with $\text{V}(\text{CO})_6$ and $\text{V}(\text{C}_6\text{H}_6)_2$ have been undertaken in order to elucidate a common structure.

Substitution of TCNE with TCNQ (7,7,8,8-tetracyano-*p*-quinodimethane),¹⁴ 2,3,5,6-tetracyanopyrazine (TCNP),¹⁵ and 2,3,5,6-tetracyanobenzene (TCNB)¹⁶ led to magnets with reduced magnetic ordering temperatures. Based on previous proposed structures of $\text{V}(\text{CO})_6$ with TCNQ, TCNE and TCNP, TCNB,¹⁷ we hypothesize the reaction between DCNT and $\text{V}(\text{CO})_6$ forms $\mu\text{-}[\text{DCNT}]^{\cdot-}$ bridging two V^{II} sites. Unfortunately the $\text{V}[\text{DCNT}]_x$ product is amorphous and the structure is unable to be determined.

The reaction between DCNT and TDAE in acetonitrile gave a grey-light pink precipitate that exhibited a sharp ν_{CN} absorption at 2222 cm^{-1} , 1669 s , 1652 s , and ν_{CH} 1409 s , 1399 s , 1386 s (Figure 2.5). The shift to lower frequency seen in the nitrile region, as was seen in the $[\text{FeCp}^*_2][\text{DCNT}]$ product, indicates reduced DCNT. The sharp bands observed at 1669 and 1652 cm^{-1} are indicative of TDAE being in the $2+$ oxidation state,¹⁸ hence the formation of the salts of the $[\text{TDAE}]^{2+}[\text{DCNT}]_2^-$ is probable. This is not

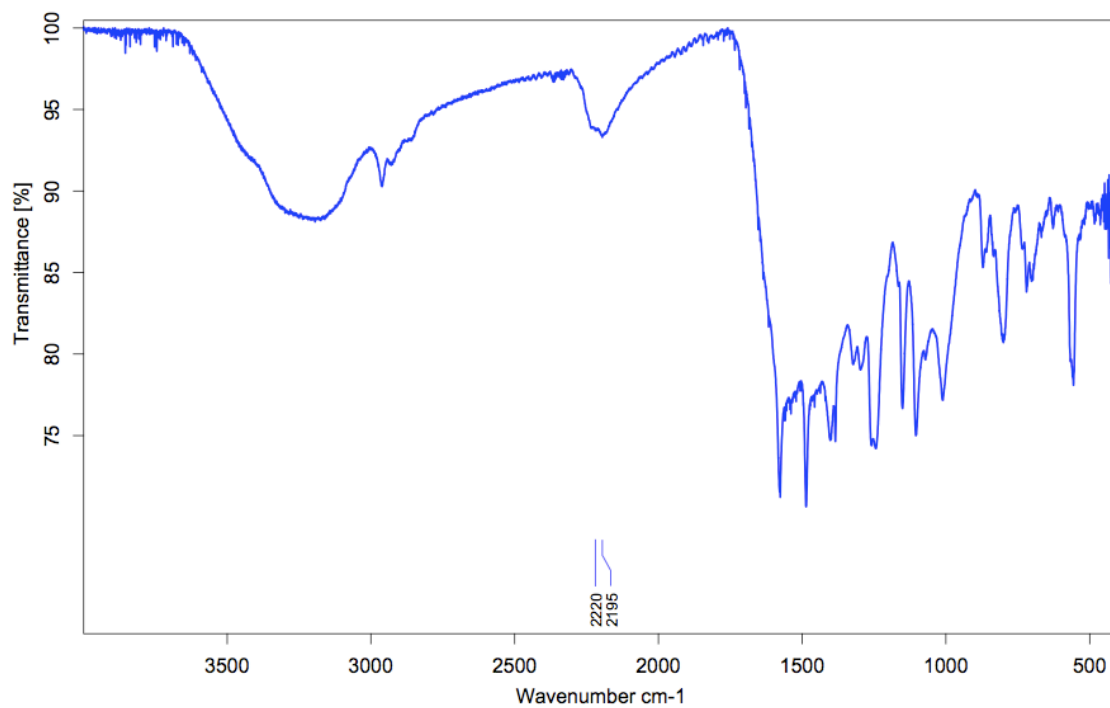


Figure 2.4. Infrared Spectrum of $V[DCNT]_x$.

surprising as TCNE and TCNQ are known to form salts of $[\text{TDAE}]^{2+}[\text{TCNQ}]_2^{2-}$, $[\text{TDAE}]^{2+}[\text{TCNQ}]^{2-}$, $[\text{TDAE}]^{2+}[\text{TCNE}]_2^{2-}$, and $[\text{TDAE}]^{2+}[\text{TCNE}]$.¹⁹ Powder X-ray diffraction at Brookhaven National Laboratory is currently being done on the sample in order to elucidate the structure.

Magnetic studies

The temperature-dependent magnetic susceptibility, χ , data were measured from 2 to 300 K, and are plotted as $\chi T(T)$ and $\chi^{-1}(T)$. $[\text{FeCp}^*_2][\text{DCNT}]$. The room-temperature χT value for $[\text{FeCp}^*_2][\text{DCNT}]$ is 0.222 emuK/mol, which is substantially lower than the calculated spin-only value of 0.75 emuK/mol for a system of two $S = 1/2$ ions or 0.375 emuK/mol for one $S = 1/2$ ion (Figure 2.6). These data are unexpected and disputes the hypothesis that the reaction between $\text{Fe}(\text{Cp}^*)_2$ and DCNT forms parallel chains, alternating between organic radical anions and $\text{Fe}(\text{Cp}^*)_2$ cations. Instead, DCNT may dimerize or trimerize but additional analysis is needed. To date, the structure of $[\text{FeCp}^*_2][\text{DCNT}]$ has not been elucidated and further investigation is needed.

$\text{V}[\text{DCNT}]\cdot\text{zCH}_2\text{Cl}_2$. Magnet data are inconclusive (Figure 2.7). $[\text{TDAE}][\text{DCNT}]$.

Magnet data are inconclusive (Figure 2.8).

Electrochemical studies

The electrochemistry of DCNT was studied by cyclic voltammetry of a 1 mM solution in MeCN (with 0.1 M $[\text{NBu}_4][\text{PF}_6]$ supporting electrolyte). An irreversible one-electron reduction is observed at -33 mV vs. SCE (Figure 2.9). This is in contrast with the report of reversible reductions at -94 (MeCN) and -81 mV (MeCN).⁶ The irreversible

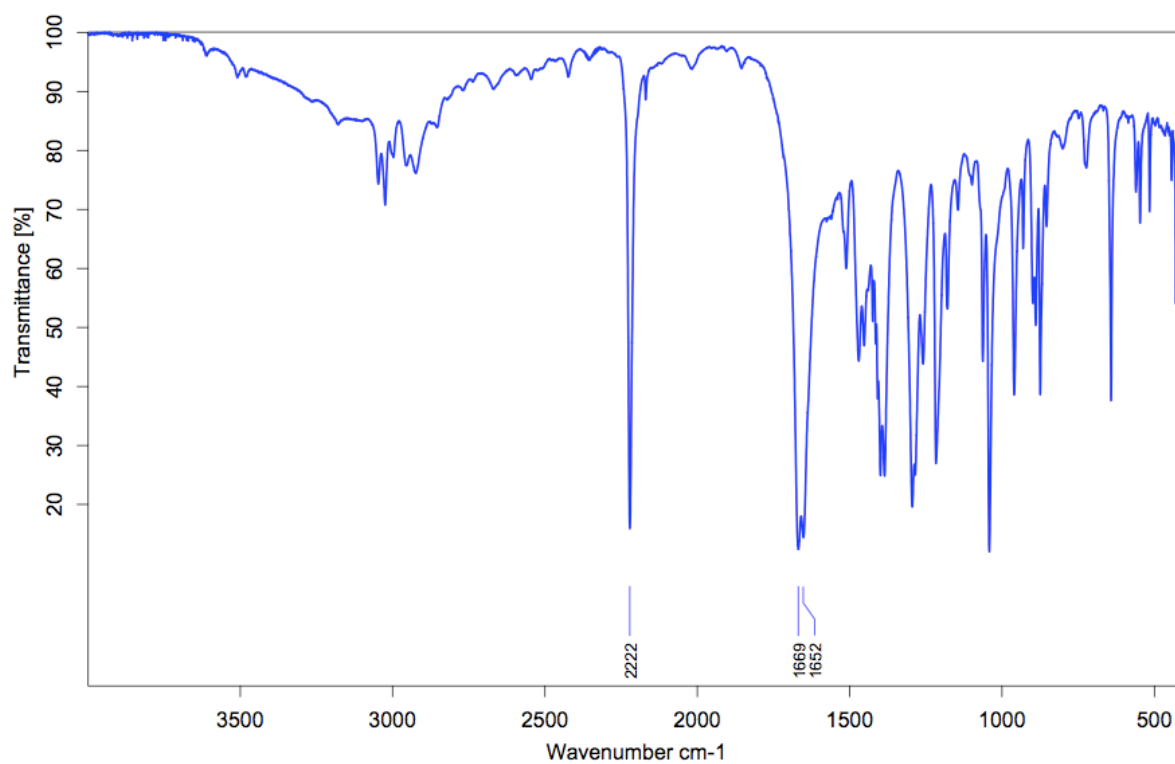


Figure 2.5. Infrared Spectrum of [TDAE][DCNT].

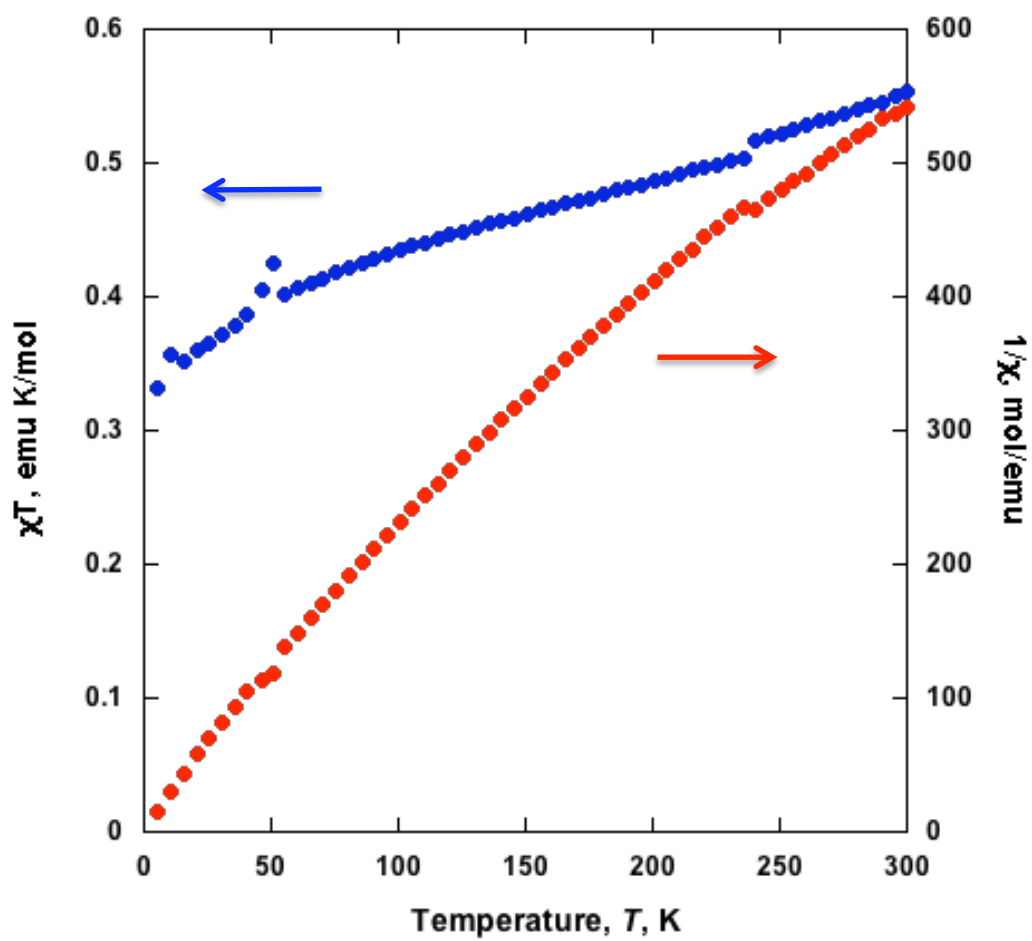


Figure 2.6. $\chi T(T)$ and $1/\chi(T)$ for $[\text{FeCp}^*_2][\text{DCNT}]$.

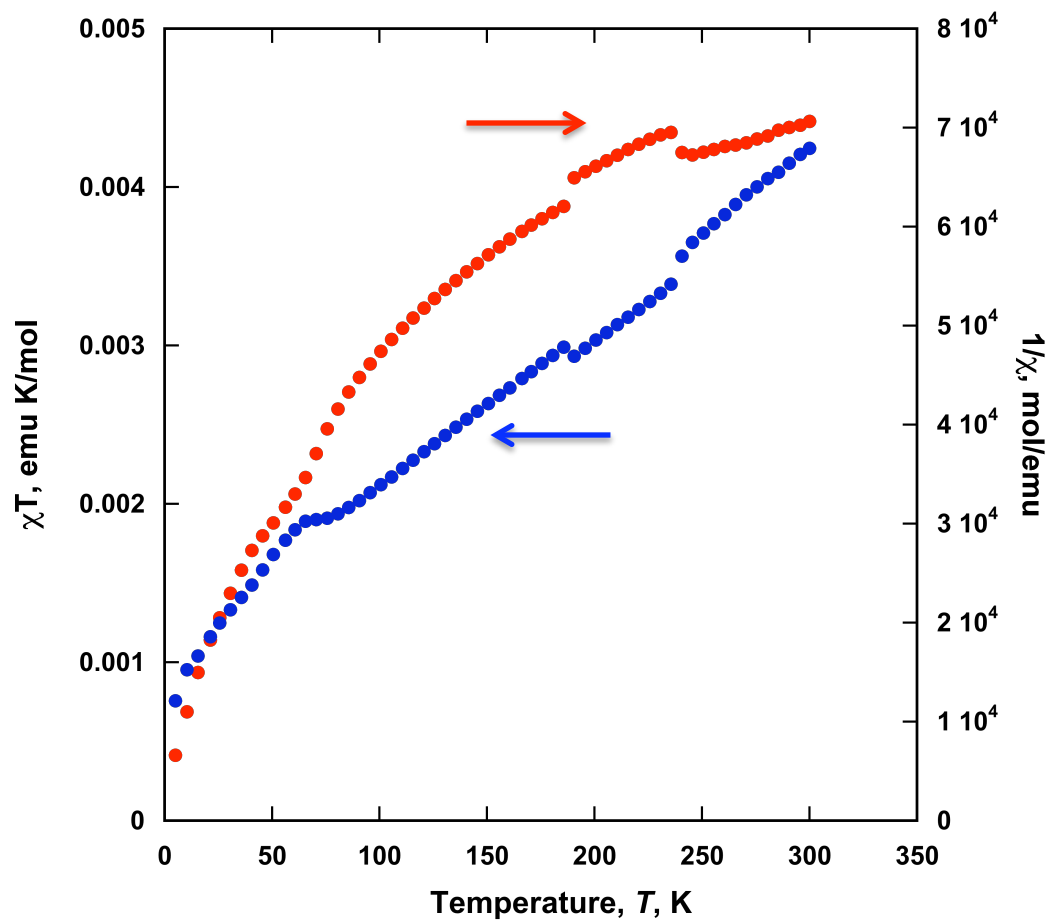


Figure 2.7. $\chi T(T)$ and $1/\chi(T)$ for $V[DCNT]_x$.

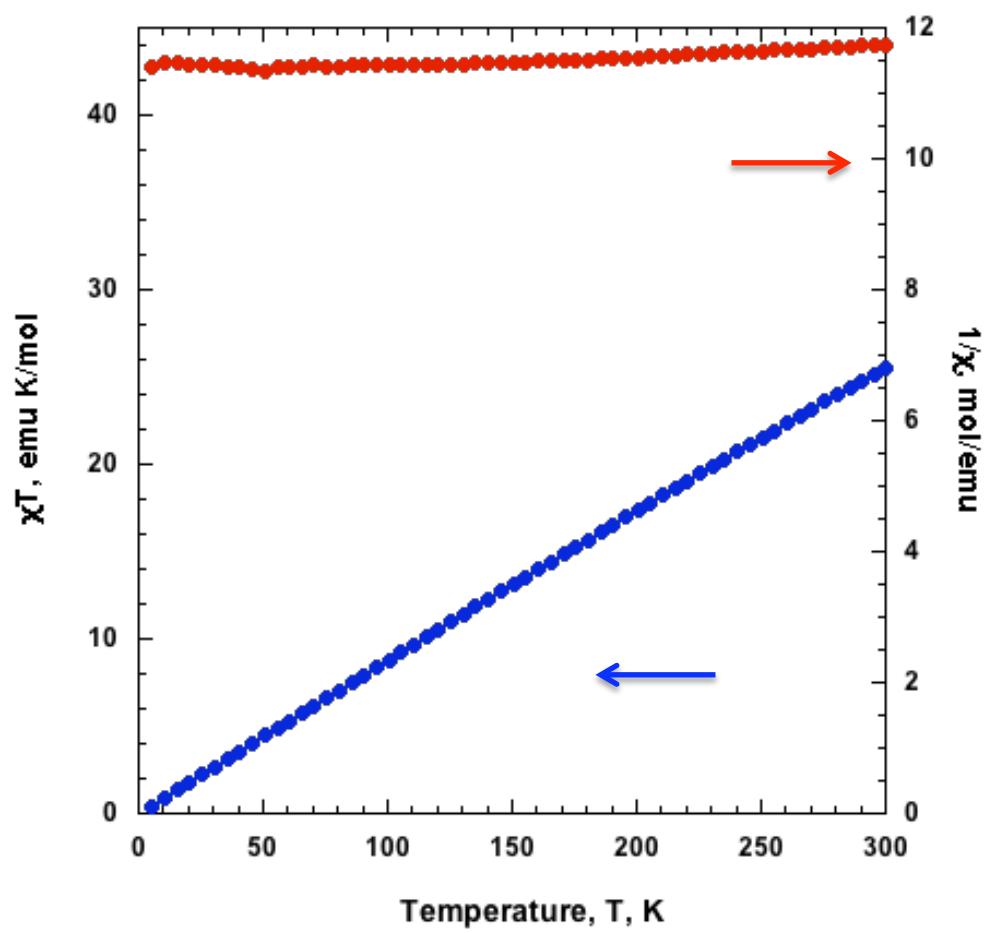


Figure 2.8. $\chi T(T)$ and $1/\chi(T)$ for [TDAE][DCNT].

reduction of DCNT can possibly be explained through the process of dimerization, and suggests that the DCNT radical anion is not stable and could immediately dimerize to $[\text{DCNT}]_2^{2-}$. This intermediate could further decompose, or polymerize. Due to this potentially happening, DCNT is unlikely to lead to new molecule-based magnets.

UV-Vis

The UV-vis spectra of DCNT (MeCN and nujol), and 1,2,4,5-tetrazine-3,6-dicarboxamide (DMF) were obtained (Figure 2.10). The absorption spectrum of a 0.1 mM solution of orange-red DCNT in MeCN showed a broad peak at $46,000\text{ cm}^{-1}$ and smaller peaks at $36,000\text{ cm}^{-1}$ and $21,000\text{ cm}^{-1}$. Its precursor, an air stable, bright magenta colored compound, 1,2,4,5-tetrazine-3,6-dicarboxamide, has a very broad absorption band at $35,000\text{ cm}^{-1}$ and $21,000\text{ cm}^{-1}$. The absorption band in the visible region at $21,000\text{ cm}^{-1}$, seen in both compounds, is typical of a tetrazine ring.⁴

Structure

The structure of DCNT and was determined by Atta Arif at the University of Utah. DCNT is planar exhibiting D_{2h} symmetry (Figure 2.11) with C-C, C-N, and N-N distances of 1.447(2), 1.3392(11), and 1.3232(16) Å, respectively. These are indicative of the expected aromatic system. In addition, DCNT packs in a herringbone motif (Figure 2.12).

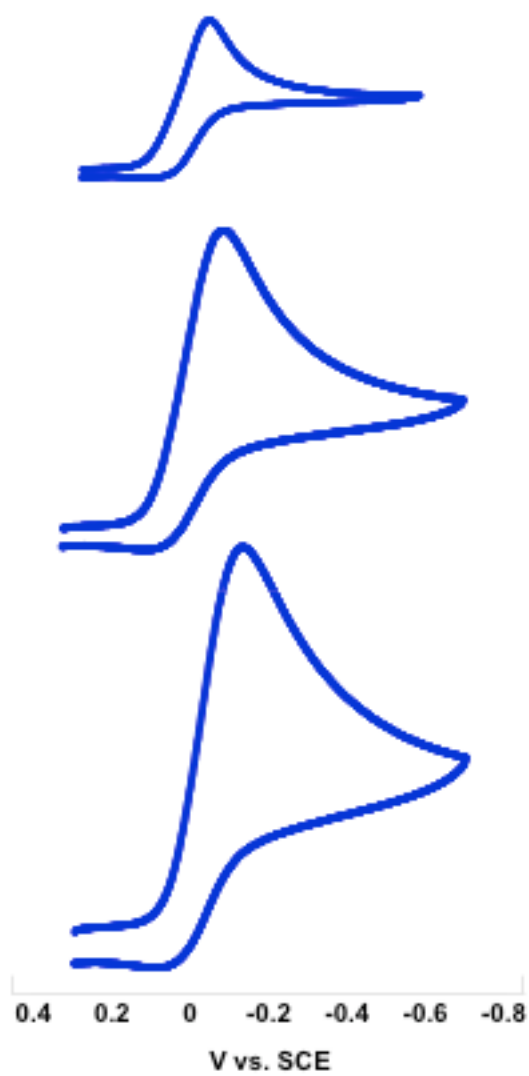


Figure 2.9. Cyclic voltammograms for DCNT at 100, 400, and 800 mV/s revealing that it undergoes an irreversible one-electron reduction.

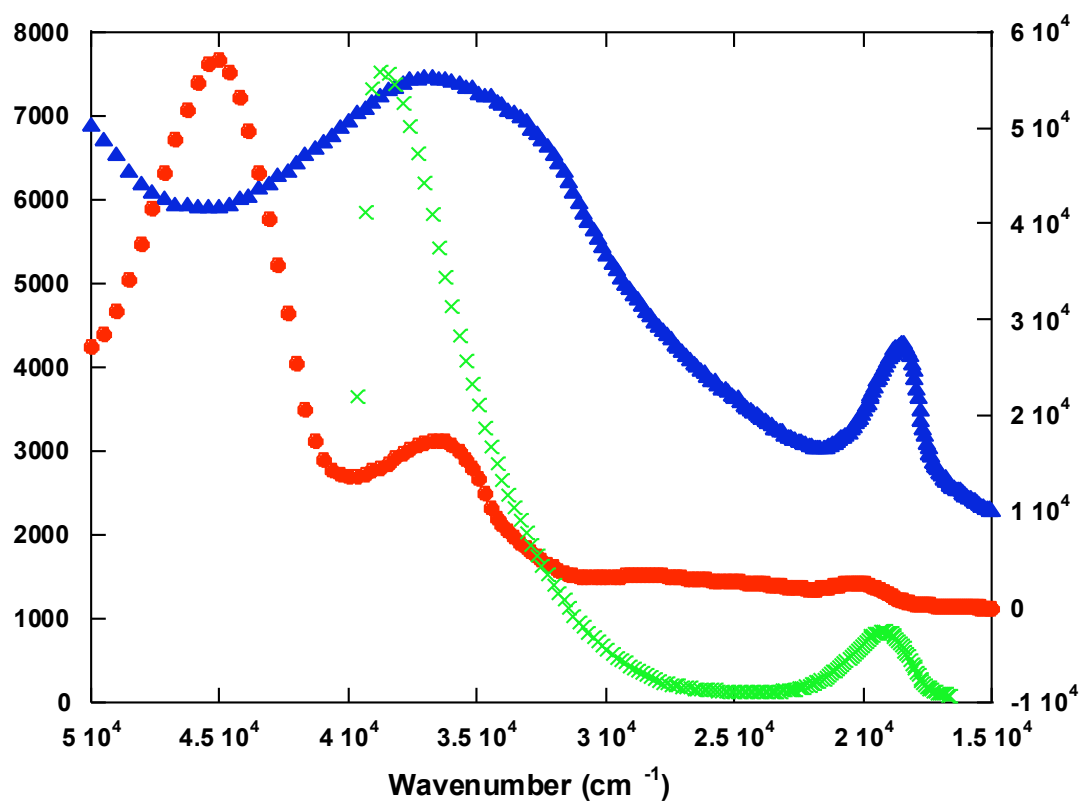


Figure 2.10. UV-vis spectra of **DCNT** (●) in MeCN, and 1,2,4,5-tetrazine-3,6-dicarboxamide in DMF (▲) and Nujol (x).

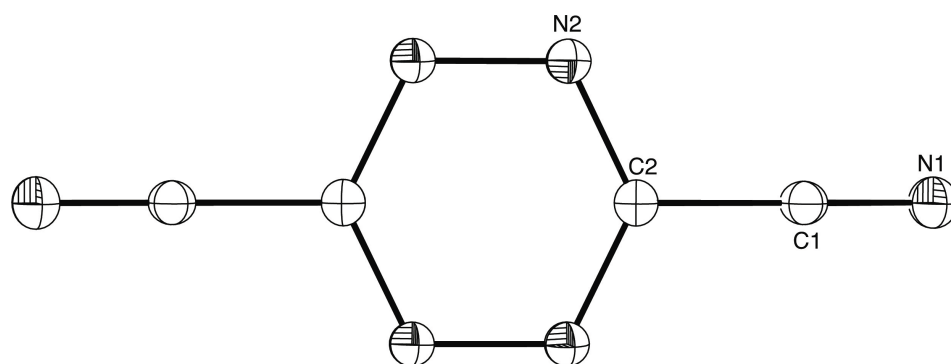


Figure 2.11. Atom labeling and thermal ellipsoid plot of DCNT.

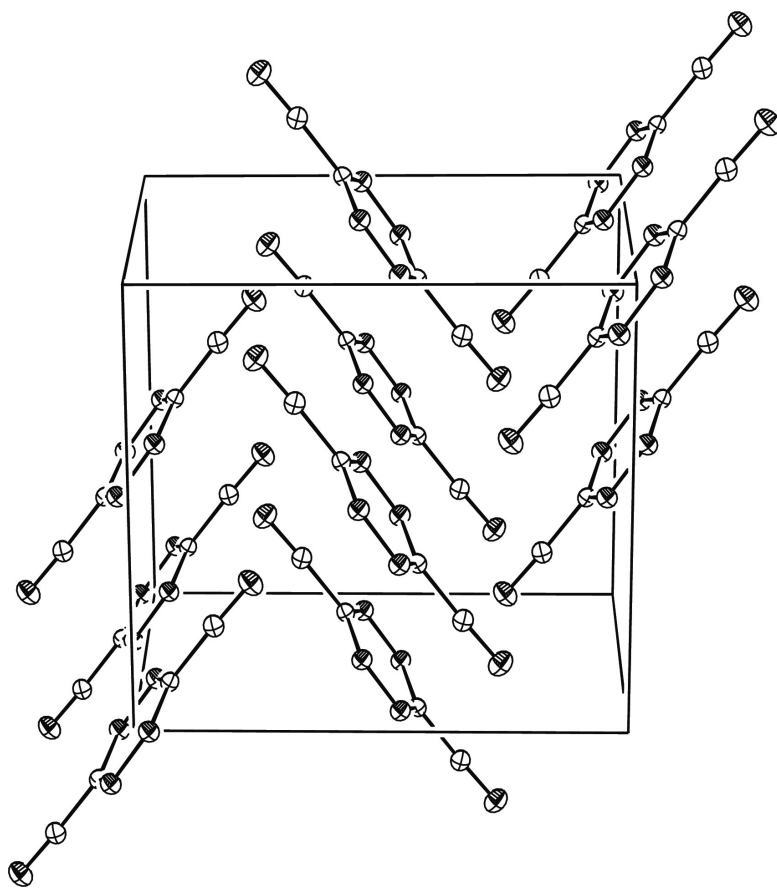


Figure 2.12. Interleaving herringbone packing motif of DCNT.

Conclusion

DCNT was successfully synthesized and characterized. Literature reported a reversible reduction potential of -0.094 V vs. SCE, which highlighted DCNT as a potential candidate in forming new molecule-based materials. This was studied via the synthesis and characterization of DCNT and from reactions of DCNT with decamethylferrocene, vanadium hexacarbonyl, and tetrakisdimethylaminoethylene. While the infrared data for each of these reactions was promising, our findings that DCNT undergoes an irreversible reduction may shed light into inconclusive magnetic data.

The reaction of $[\text{FeCp}^*_2][\text{DCNT}]$ showed promising results as the infrared spectra indicated reduced DCNT. Thus, suggesting DCNT is closely correlated to other similar cyanocarbon accepts such as TCNE and TCNQ, which, when reacted with $\text{Fe}(\text{Cp}^*)_2$, form parallel chains of alternating radical cations and planar radical organic anions. However, the magnetic data does not corroborate this hypothesis. Another bonding motif may be occurring that could include the dimerization or trimerization of DCNT and further analysis needs to be done. Our collaborators are currently trying to elucidate the structure via powder X-ray diffraction. While the magnet data for $\text{V}[\text{DCNT}]_x$ and $[\text{TDAE}][\text{DCNT}]$ are inconclusive, the infrared data indicates that DCNT is well-suited to forming charge transfer salts. The infrared spectra for both $\text{V}[\text{DCNT}]_x$ and $[\text{TDAE}][\text{DCNT}]$ denote reduced DCNT. In addition, the infrared spectrum of $[\text{TDAE}][\text{DCNT}]$ indicates the presence of TDAE in the 2+ oxidation. These electron transfer salts may have applications as molecular-based, metal like conductors.

References

- (1) Miller, J. S. *Angew. Chem. Int. Ed.* **2006**, *45*, 2508 – 2525.
- (2) Miller, J. S.; Calabrese, J. C.; Rommelmann, H.; Chittipeddi, S. R.; Zhang, J. H.; Reiff, W. M.; Epstein, A. J. *J. Am. Chem. Soc.* **1987**, *109*, 769-781.
- (3) Manriquez, J. M.; Yee, T. G.; Mclean, R. S.; Epstein, A. J.; Miller, J. S. *Science*, **1991**, *252*, 1415-1416.
- (4) (a) Fitzgerald, J. P.; Kaul, B. B.; Yee, G. T. *Chem. Comm.* **1999**, *2000*, 49-50. (b) Vickers, E. B.; Shelby, T. S.; Miller, J. S. *J. Am. Chem. Soc.* **2004**, *126*, 3716-3717. (c) Vickers, E. B.; Shelby, T. S.; Thorum, M. S.; Taliaferro, M. L.; Miller, J. S. *Inorg. Chem.* **2004**, *43*, 6414-6420.
- (5) Kaim, W. *Coord. Chem. Rev.* **2002**, *230*, 127-139.
- (6) Gleiter, R.; Schehlmann, V.; Spanget-Larsen, J.; Fischer, H.; Neugebauer, F. A. *J. Org. Chem.* **1988**, *53*, 5756.
- (7) Bond, A. M.; Colton, R. *Inorg. Chem.* **1976**, *15*, 2036-2040.
- (8) Richmond, T. G.; Shi, Q.; Trogler, W. C.; Basolo, F. *J. Am. Chem. Soc.* **1984**, *106*, 76-81.
- (9) Liu, X.; Ellis, J. E.; Selby, T. D.; Ghalsasi, P.; Miller, J. S. *Inorg. Synth.* **2004**, *34*, 68.
- (10) (a) Boger, D. L.; Coleman, R. S.; Panek, J. S.; Huber, F. X.; Sauer, J. *J. Org. Chem.*, **1985**, *50*, 5377–5379. (b) *J. Org. Chem. Soc.* 1952, *17*, 381-389. (c) Berlin, A.; Pagni, G. A.; Sanniccolo, F. *Synthetic Metals*, **1987**, *19*, 415-418.
- (11) Miller, J. S.; Zhang, J. H.; Reiff, W. H.; Dixon, D. A.; Preston, L. D.; Reis, A. H.; Gebert, E.; Extine, M.; Troup, J. *J. Phys. Chem.*, **1987**, *91*, 4344–4360.
- (12) Miller, J. S. *J. Mater. Chem.* **2010**, *10*, 1846-1857.
- (13) Arthur, J. L.; Lapidus, S. H.; Moore, C. E.; Rheingold, A. L.; Stephens, P. W.; Miller, J. S. (2012), *Adv. Funct. Mater.*
- (14) Vickers, E. B.; Shelby, T. S.; Thorum, M. S.; Taliaferro, M. L.; Miller, J. S. *Inorg. Chem.* **2004**, *43*, 6414–6420.
- (15) E. B. Vickers, T. D. Selby, J. S. Miller, *J. Am. Chem. Soc.* **2004**, *126*, 3716.

- (16) Taliaferro, M. L.; Thorum, M. S.; Miller, J. S. *Angew. Chem. Int. Ed.* **2006**, *45*, 5326–5331.
- (17) (a) Taliaferro, M. L.; Thorum, M. S.; Miller, J. S. *Angew. Chem. Int. Ed.* **2006**, *45*, 5326–5331. (b) Vickers, E. B.; Shelby, T. S.; Miller, J. S. *J. Am. Chem. Soc.* **2004**, *126*, 3716–3717. (c) Vickers, E. B.; Shelby, T. S.; Thorum, M. S.; Taliaferro, M. L.; Miller, J. S. *Inorg. Chem.* **2004**, *43*, 6414–6420. (d) Manriquez, J. M.; Yee, T. G.; Mclean, R. S.; Epstein, A. J.; Miller, J. S. *Science*, **1991**, *252*, 1415–1416.
- (18) Pokhodnia, K. I.; Papavassilio, J.; Umek, P.; Omerzu, A.; Mihailovic, D. *J. Chem. Phys.* **1999**, *110*, 3606–3611.
- (19) Fox, J. R.; Foxman, B. M.; Guarrera, D.; Miller, J. S.; Calabrese, J. C.; Reis, A. H. *J. Mater. Chem.* **1996**, *6*, 1627–1631.
- (20) Audebert, P.; Sadki, S.; Miomandre, F.; Clavier, G. *Electrochem. Commun.* **2004**, *6*, 144–147.